Evaporative cooling of unitary Fermi gas mixtures in optical traps

L Luo, B Clancy, J Joseph, J Kinast, A Turlapov and J E Thomas

Physics Department, Duke University, Durham, NC 27708-0305, USA
E-mail: jet@phy.duke.edu

Abstract. We measure the scaling laws for the number of atoms and the cloud size as a function of trap depth for evaporative cooling of a unitary Fermi gas in an optical trap. A unitary Fermi gas comprises a trapped mixture of atoms in two hyperfine states which is tuned to a collisional (Feshbach) resonance using a bias magnetic field. Near resonance, the zero energy s-wave scattering length diverges, and the s-wave scattering cross-section is limited by unitarity to be $4\pi/k^2$, where k is the relative wavevector of the colliding particles. In this case, the collision cross-section for evaporation scales inversely with the trap depth, enabling runaway evaporation under certain conditions. We demonstrate high evaporation efficiency, which is achieved by maintaining a high ratio η of trap depth to thermal energy as the trap depth is lowered. We derive and demonstrate a trap lowering curve which maintains η constant for a unitary gas. This evaporation curve yields a quantum degenerate sample from a classical gas in a fraction of a second, with only a factor of three loss in atom number.

Contents

1. Introduction

Evaporative cooling in all-optical traps provides a simple and efficient method for producing degenerate Bose [1] and Fermi [2, 3] gases. In these all-optical cooling experiments, an optical dipole trap is directly loaded from a magneto-optical trap (MOT) containing precooled atoms, and then forced evaporation is initiated in the optical trap by lowering the trapping laser intensity. All-optical methods have now been used to produce BECs of ^{87}Rb [1], ^{137}Cs [4], ^{23}Na [5], and diatomic molecular ^{6}Li [6], as well as degenerate Fermi gases of ^{6}Li [2, 7, 8]. Evaporation in optical dipole traps is currently being used in studies of strongly interacting Fermi gas mixtures, both by direct loading from an MOT [7, 8] and after initial evaporative cooling in a magnetic trap [9]–[12].

Strongly interacting Fermi gases are produced using a mixture of atoms in two hyperfine states, denoted as 'spin-up and spin-down,' which is magnetically tuned to a collisional (Feshbach) resonance. Near the resonance, the zero energy s-wave scattering length for particles of opposite spin far exceeds the interparticle spacing, producing a strongly interacting gas. Strongly interacting Fermi gas mixtures are of great interest, since they serve as models to test non-perturbative many-body theories of exotic systems in nature, from very high temperature superconductors to neutron stars and quark–gluon plasmas [3, 13].

Near resonance, the magnitude of the scattering amplitude (for collisions between Fermi atoms of different spin) reaches the maximum permitted by unitarity, i.e., $1/k$, where k is the relative wavevector of the colliding particles. For a degenerate Fermi gas, the interparticle spacing determines the scale of $1/k = 1/k_F$, where k_F is the Fermi wavevector. The resulting large collision cross-section enables rapid evaporation of the strongly interacting gas to quantum degeneracy [7].

In this paper, we study forced evaporative cooling of a unitary Fermi gas which is contained in an optical trap that is continuously lowered. Under some conditions, the unitary gas enables runaway evaporative cooling, i.e., an increase in the collision rate with decreasing trap depth, which arises from the increase in the scattering cross-section with decreasing relative kinetic energy. By contrast, for evaporative cooling of a gas with an energy-independent scattering cross-section, the collision rate always decreases as the trap is lowered [14]. We measure the scaling laws for the atom number and cloud size during forced evaporation of a unitary Fermi gas in a continuously lowered optical trap, and show that they are consistent with our predictions.

Efficient evaporation is obtained when the ratio η of the trap depth U to the thermal energy $k_B T$ is large. When inelastic processes are not important, the large value of η assures that evaporating atoms carry away a large amount of energy compared to the average thermal energy, assuring high efficiency, i.e., a large fraction of the initial atom number remains when degeneracy is achieved. Although the evaporation rate is suppressed by the Boltzmann factor $\exp(-\eta)$, for an optically trapped gas, the collision rate is very high so that typically $\eta = U/k_B T$ can be ten or more, but it may vary during the evaporation sequence. For an arbitrary time-dependent trap lowering curve $U(t)$, η is not generally constant. However, by considering the evaporation rate, it is possible to lower the optical trap so that η is held at a constant large value [14]. For any constant value of η, it is easy to obtain analytic results for the scaling laws and for the trap lowering curve [14], as described below for the unitary gas in section 4.

2. Scaling laws

We begin by reviewing the scaling laws. The optical trapping potential can be written generally as

$$V(\mathbf{x}, t) = -U(t)g(\mathbf{x}), \tag{1}$$

where $g(\mathbf{x})$ describes the trap shape, with $g(0) = 1$ and $g(|\mathbf{x}| \to \infty) \to 0$. We assume that evaporation is carried out at low temperatures near stagnation, where the average thermal energy $kT \ll U$, with $U \equiv U(t)$.

The scaling laws easily follow from energy conservation, with the assumption of constant η. The trapped gas loses energy at a rate $\dot{E}$ by evaporation and by the work done as the trapping potential is lowered. For $kT \ll U$, the atoms are approximately in a harmonic potential, so that

$$\dot{E} = \frac{\dot{U}}{U}\frac{E}{2} + \dot{N}(U + \alpha kT). \tag{2}$$

Here, the first term arises from the change in the harmonic potential energy. The second term arises from the evaporation rate, so that $\dot{N} < 0$. $U + \alpha k_B T$ is the average energy carried away per particle.

In general, $0 \leqslant \alpha \leqslant 1$ [15]. For example, using an energy-independent s-wave scattering cross-section, we find $\alpha = (\eta - 5)/(\eta - 4)$ for any potential which is harmonic near the minimum.[1] The value of α is nearly the same for a unitary gas, because the relative kinetic energy that appears in the collision cross-section is determined by the trap depth U, as discussed below. Hence, the cross-section is nearly constant in the collision integral, and can be factored out, so that the ratio of the evaporative energy loss to the number loss is essentially unchanged from that of an energy-independent cross-section.

For evaporative cooling from the classical regime to degeneracy, we can take the total energy to be that of a classical gas in a harmonic potential, $E = 3Nk_B T$. Using this in equation (2) for

---

[1] Note that the s-wave Boltzmann equation contains the trapping potential explicitly only in the density of states $\mathcal{D}(\epsilon_{min})$ [15]. For evaporation, it can be shown that $\epsilon_{min} \simeq kT \ll U$, so that $\mathcal{D}(\epsilon_{min})$ can be approximated by the harmonic oscillator result $\propto \epsilon_{min}^2$.

fixed η, one readily obtains the atom number scaling,

$$\frac{N}{N_0} = \left(\frac{U}{U_0}\right)^{\frac{3}{2(\eta'-3)}},$$ (3)

where the subscript 0 denotes the initial conditions at $t = 0$ and $N = N(t)$. Here, $\eta' = \eta + \alpha = \eta + (\eta - 5)/(\eta - 4)$.

We can also determine how the phase space density scales. The phase space density per spin state in the classical regime is essentially the fugacity per spin state, or, for a 50–50 mixture of two spin states, just $N/2$ divided by the total number of accessible harmonic oscillator states, i.e., $\rho = (N/2)(h\bar{\nu}/k_B T)^3$, where $\bar{\nu} \equiv (\nu_x \nu_y \nu_z)^{1/3}$. Using $\bar{\nu} \propto \sqrt{U}$ and $k_B T \propto U$, with equation (3), we obtain

$$\frac{\rho}{\rho_0} = \left(\frac{U_0}{U}\right)^{\frac{3(\eta'-4)}{2(\eta'-3)}} = \left(\frac{N_0}{N}\right)^{\eta'-4}.$$ (4)

The evaporation efficiency χ is very high for optical traps with large η, according to equation (4):

$$\chi = \frac{\ln(\rho/\rho_0)}{\ln(N_0/N)} = \eta' - 4.$$ (5)

While $\chi \leqslant 3$ is typical for BECs produced in magnetic traps [16], for $\eta = 10$, equation (5) yields $\chi = 6.83$. Hence, in optical traps, a quantum degenerate gas is produced with little reduction in atom number, as demonstrated below.

For a fixed value of η, the mean square cloud size in the trap does not change. This follows from the scaling of the total energy, which is six times the potential energy for one direction, x, i.e., $E = 3NM\omega_x^2 \langle x^2 \rangle_{\text{trap}}$. Note that this result is a consequence of the virial theorem, and holds generally for both a unitary gas and an ideal gas in a harmonic trap [17]. Here, M is the atom mass and ω_x is the harmonic oscillation frequency of an atom in the x-direction. We assume a harmonic approximation to a gaussian trap, where the trapping potential takes the form $U(t)(1 - \exp(-2x^2/a_x^2)) \simeq M\omega_x^2(t) x^2/2$, and similarly for the y-direction, with a_x the trap field $1/e$ radius in the x-direction, i.e., the intensity $1/e^2$ radius. Then, both the energy $E = 3Nk_B T = 3NU/\eta$ and the spring constant $M\omega_x^2 = 4U/a_x^2$ are proportional to U. Hence, the mean square radius of the trapped cloud does not change as the trap is lowered with a constant value of η, and

$$\langle x^2 \rangle_{\text{trap}} = \frac{a_x^2}{4\eta},$$ (6)

remains constant.

3. Experiments

Our experiments employ a 50–50 mixture of the two lowest hyperfine states of ^{6}Li fermions, which is confined in a stable CO_2 laser trap [18]. The mixture exhibits a Feshbach resonance at 834 G for which the s-wave scattering length diverges [19], producing a unitary gas where the scattering cross-section is inversely proportional to the relative kinetic energy.
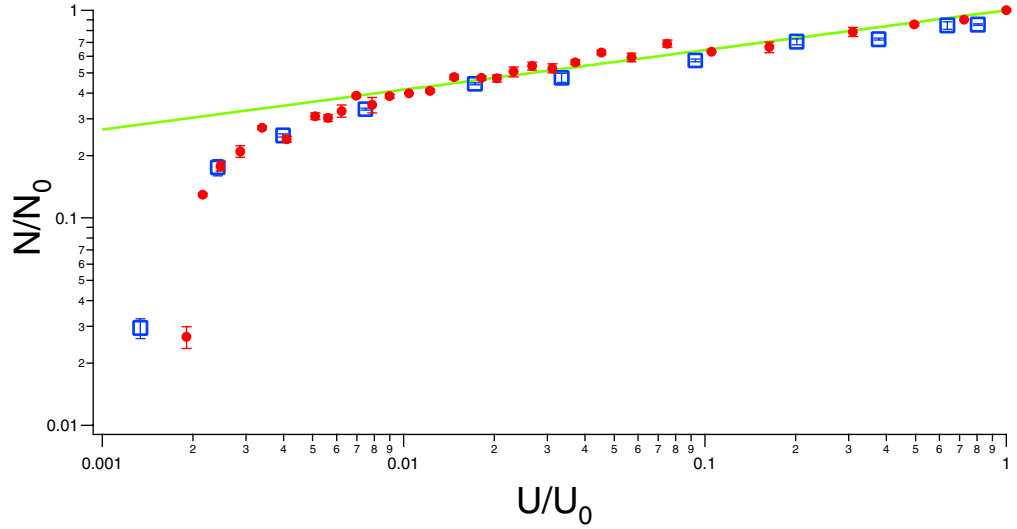
Figure 1. Atom number versus trap depth. The solid green line shows the scaling law prediction for $\eta = U/k_B T = 10$. Note that the data deviate from the scaling law prediction when the gas becomes degenerate, near $U/U_0 = 0.007$. Red solid circles: obtained using a trap lowering curve for an energy-independent scattering cross-section. Blue open squares: obtained using the trap lowering curve for unitary gas. Note that trap lowering time increases from right to left.

The maximum laser power P_0 at the trap focus is between 50 and 60 W. Parametric resonance measurements in the weakly interacting regime at low magnetic field yield typical harmonic oscillator frequencies at full trap depth U_0, $\omega_x = 2\pi\nu_x = 2\pi \times 5500$ Hz, $\omega_y = 2\pi\nu_y = 2\pi \times 5400$ Hz, and $\omega_z = 2\pi\nu_z = 2\pi \times 190$ Hz.

We estimate the maximum trap depth using the known power and $U_0 = 4\alpha_g P_0/(c\,a_x a_y)$, where α_g is the ground state static polarizability of ^{6}Li, 24.3×10^{-24} cm^3 [20], and $c = 3 \times 10^{10}$ cm s^{-1}. It is easy to show that for a given power, $a_x^4 = 4(\nu_y/\nu_x^3)\alpha_g P_0/(\pi^2 Mc)$, where $M = 1.0 \times 10^{-23}$ g is the atom mass, and $a_y = a_x\nu_x/\nu_y$. Assuming $P_0 = 60$ W, we obtain $a_x = 50.3\,\mu$m, $a_y = 51.2\,\mu$m, and $U_0/k_B = 550\,\mu$K. For $P_0 = 50$ W, the estimated spot sizes are reduced by a factor of 0.96, and the estimated trap depth is $500\,\mu$K.

The CO_2 laser trap is directly loaded from a ^{6}Li MOT. Typically, the total number of atoms is 2×10^6. The magnetic field is ramped to the Feshbach resonance and the atoms are allowed to evaporate at fixed trap depth, yielding $N_0 = 8 \times 10^5$ at stagnation. The trap is then lowered by a factor $U(t)/U_0$.

Figure 1 shows how the observed total number of atoms N/N_0 scales with trap depth U/U_0 for two different trap lowering curves, shown in red solid circles and blue open squares, which are described in detail in section 4. Note that trap lowering time increases from right to left. Fitting $N/N_0 = (U/U_0)^p$, we obtain $p = 0.21(0.01)$. For $\eta = 10$, equation (3) predicts $p = 0.191$, which is shown as the solid line. The scaling law is obeyed down to about 1% of the maximum trap depth, where the Fermi gas becomes degenerate and the scaling law fails, as discussed further below.

We also measure the transverse cloud size after release and subsequent expansion for a time t_{exp}, which is between 400 and 1200 μs. The measured transverse cloud size is found to scale

Institute *of* **Physics** ⏀ DEUTSCHE PHYSIKALISCHE GESELLSCHAFT
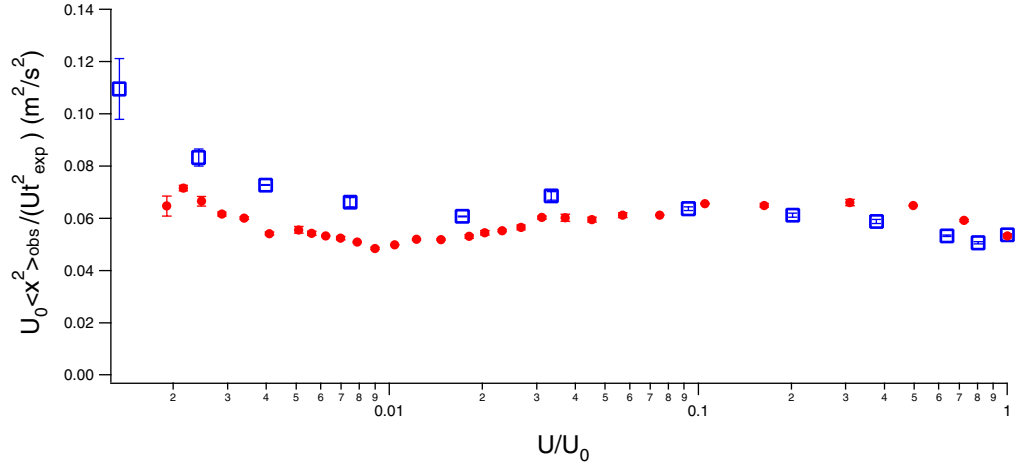
Figure 2. Mean square cloud size in the trap, which is nearly independent of trap depth. Red solid circles: obtained using the trap lowering curve for an energy-independent scattering cross-section. Blue open squares: obtained using the trap lowering curve for unitary gas. Note that the trap lowering time increases from right to left.

linearly with trap depth U and quadratically with expansion time t_{exp}, the result expected for a trapped cloud radius which is independent of U, as we now show.

The size of the observed expanded cloud is related to that of the trapped gas by a scale factor, i.e., $\langle x^2 \rangle_{obs} = b_x^2(t_{exp}) \langle x^2 \rangle_{trap}$. A unitary gas expands hydrodynamically, by a known scale factor $b_x(t_{exp})$ [7, 21]. However, when $\omega_x t_{exp} \gg 1$, the difference between the hydrodynamic and ballistic expansion factors is nearly constant. Hence, we take $b_x^2(t) \simeq (\omega_x t)^2$. Using $\omega_x^2 = 4U/Ma_x^2$ and equation (6), we see that

$$\frac{\langle x^2 \rangle_{obs}}{(U/U_0)t_{exp}^2} = \frac{U_0}{\eta M} \tag{7}$$

should be nearly independent of U/U_0.

Figure 2 shows the data corresponding to the left-hand side of equation (7). We find that the ratio $\langle x^2 \rangle_{obs}/[(U/U_0) t_{exp}^2] \simeq 0.06 \, \mathrm{m^2 \, s^{-2}}$ is nearly constant, as expected for a constant value of η. Equation (7) shows that $U_0 = 0.06 \, \eta M$. Using $\eta = 10$ from the number scaling, we find that $U_0/k_B = 440 \, \mu\mathrm{K}$, comparable to the above estimates which are based on the measured trap oscillation frequencies and power.

4. Trap depth lowering curve for a unitary gas

The data show that the scaling laws are reasonably well obeyed. We now derive the ideal trap depth lowering curve for maintaining η constant in a unitary gas, which differs from that obtained previously for an energy-independent collision cross-section [14].

We begin by determining the collision cross-section for atoms which evaporate from the trap in the unitary regime. This can be done using the Boltzmann equation for an energy-dependent

cross-section [22]. Expanding to first order in the small parameter ϵ_s/U, where $\epsilon_s = 2\hbar^2/(Ma^2)$ and $|a| \to \infty$ near the Feshbach resonance, we obtain for a single component (Bose) gas,

$$\sigma(U) = \frac{16\pi\hbar^2}{MU}, \tag{8}$$

where we neglect $k_B T$ compared to U, assuming large η. This result is readily obtained by the following heuristic arguments. For a collision between two particles of energies ϵ_1 and ϵ_2, energy conservation dictates that $\epsilon_1 + \epsilon_2 = \epsilon_3 + \epsilon_4$, where ϵ_3 and ϵ_4 are the energies of the outgoing particles. For evaporation, we require that $\epsilon_4 > U$, the trap depth, while ϵ_3 is reduced in energy. Then, we must have $\epsilon_3 \leqslant k_B T$, to avoid significantly decreasing the Boltzmann factor $\exp(-\eta)$, which for evaporation is already small. Since $\epsilon_3 = Mv_3^2/2 + U(x_c)$, with $U(x_c)$ the harmonic trap potential energy at the collision point x_c, we must have $U(x_c) \leqslant k_B T \ll U$, and we can take $Mv_3^2/2 \to 0$ and $U(x_c) \to 0$ compared to the trap depth U. Hence, we can take $v_3 \simeq 0$, compared to the other speeds for 1, 2, and 4. Then, one easily shows that $v_4^2 = v_1^2 + v_2^2$. Momentum conservation yields $\mathbf{v}_1 + \mathbf{v}_2 = \mathbf{v}_4$, where again we assume $v_3 = 0$. Then, squaring both sides, we see that $\mathbf{v}_1 \cdot \mathbf{v}_2 \simeq 0$ and $v_{rel}^2 \simeq v_4^2 \simeq 2U/M$. Using $Mv_{rel}/2 = \hbar k$ in the cross-section $8\pi/k^2$ yields equation (8).

To determine the trap depth lowering curve that is needed to maintain constant η in a unitary gas, we consider the evaporation rate [14]. To determine the evaporation rate, we need only to replace the constant cross-section in [14] by the unitary cross-section, $\sigma(U)$.

From the s-wave Boltzmann equation [15], we obtain the evaporation rate to lowest order in $\exp(-\eta)$. Neglecting background gas collisions for simplicity (these can be included [14]), we obtain
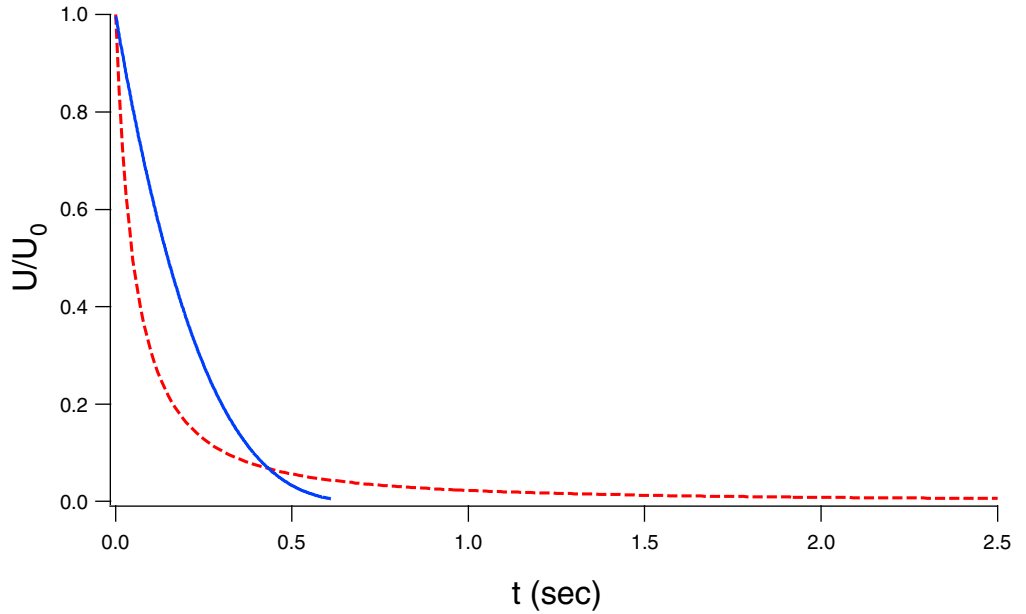
$$\dot{N} = -2(\eta - 4)\exp(-\eta)\gamma N. \tag{9}$$

The collision rate $\gamma = nv_{rel}\sigma$ scales as $Nv_{rel}\sigma$, since the cloud size does not change, so that the density scales as the number N. Since the relative speed scales as $U^{1/2}$, and the cross-section as $1/U$, we obtain

$$\frac{\gamma}{\gamma_0} = \left(\frac{U}{U_0}\right)^{\frac{6-\eta'}{2(\eta'-3)}}. \tag{10}$$

The initial collision rate γ_0 is obtained using the results given in [14], with the constant cross-section σ replaced by the unitary cross-section of equation (8). With $kT_0 = U_0/\eta$, we obtain $\gamma_0 = (N_0/4)\,64\pi^2\hbar^2\bar{v}^3\eta/(U_0^2)$, where the (1/4) arises for a Fermi gas in a 50–50 mixture of two spin states. The rate for a single component Bose gas is four times larger. In contrast to the collision rate for a constant cross-section, for $\eta' > 6$, the unitary collision rate increases as the trap depth is lowered, because the cross-section increases faster than the flux nv_{rel} decreases.

Differentiating equation (3) with respect to t and using the result in equation (9), we obtain the lowering curve for a unitary gas,

$$\frac{U(t)}{U_0} = \left(1 - \frac{t}{\tau_u}\right)^{2(\eta'-3)/(\eta'-6)}. \tag{11}$$

Institute of **Physics** Φ DEUTSCHE PHYSIKALISCHE GESELLSCHAFT

Figure 3. Trap depth U/U_0 versus time. Red dashed line: lowering curve for an energy-independent scattering cross-section. Blue solid line: lowering curve for a unitary gas. Each curve ends when $U/U_0 = 1/150$, where the gas becomes quantum degenerate.

Here, $0 \leqslant t \leqslant \tau_u$, and

$$\frac{1}{\tau_u} = \frac{2}{3}(\eta - 4)(\eta' - 6)\exp(-\eta)\gamma_0, \tag{12}$$

where γ_0 is given above. For $\eta' = 6$, one can show that the trap lowering curve is exponential.

   Our data were obtained using two different trap lowering curves. The red solid circle data in figures 1 and 2 show the results obtained using the lowering curve for an energy-independent cross-section and $\eta = 10$, $U/U_0 = 1/(1 + t/\tau)^{1.45}$ [14], where $\tau = 0.08$ s is chosen to optimize the efficiency. The corresponding blue open square data show the results obtained using the lowering curve for a unitary gas with $\eta = 10$, where $U(t)$ is calculated from equations (11) and (12), $U/U_0 = (1 - t/\tau_u)^{3.24}$, and $\tau_u = 0.77$ s. Both curves yield similar results for the number and trap size, but the unitary lowering curve is much faster, as it includes the effects of runaway evaporation which does not occur with an energy-independent cross-section.

   We can estimate the ratio U/U_0 needed to achieve degeneracy for a Fermi gas in the classical regime, assuming a 50–50 mixture of spin-up and spin-down atoms. The initial phase space density is $\rho_0 = (N_0/2)(h\bar{\nu}_0/k_B T)^3$. For our trap conditions at full depth, where $U_0 = 550\,\mu$K, we have $\bar{\nu}_0 = 1780$ Hz and $k_B T_0 = U_0/\eta = 55\,\mu$K for $\eta = 10$. With $N_0 = 8 \times 10^5$, $\rho_0 = 1.5 \times 10^{-3}$. From equation (4), with $\eta = 10$, we have $\rho = \rho_0 (U_0/U)^{1.3}$. Lowering the trap by a factor of 150 yields $\rho \simeq 1$. Figure 3 shows trap lowering curves for a gas with an energy-independent collision cross-section and for a unitary gas. We find that by using the unitary gas lowering curve, degeneracy is achieved in 0.61 s, while the optimized constant cross-section curve requires 2.45 s.

We see that the atom number data of figure 1 deviates from the scaling law predictions below $U/U_0 = 0.007 \simeq 1/150$, in good agreement with the predicted depth at which degeneracy occurs. In this regime, where the Fermi gas is degenerate, further lowering of the trap depth cuts into the Fermi surface causing increased atom loss. A different trap lowering curve is needed to optimize the efficiency in this regime, and can be determined. However, in practice, one can simply adjust the final trap depth to slightly cut into the Fermi surface.

5. Mean free path for evaporating atoms

Our derivation assumes that evaporating atoms leave the trap after a binary collision, even though the gas is unitary and the collision cross-section is large. We now show that although the gas in the trap is hydrodynamic, the cross-section for evaporating atoms to collide with trapped atoms can be sufficiently small. We consider the conditions for the mean free path to be larger than the transverse trap dimension, and determine the minimum trap depth U_c below which our assumptions are no longer strictly valid.

Consider the ratio of the mean free path $l = 1/(\bar{n}\sigma)$, at the average density $\bar{n}$, to the rms transverse trap size $d_x \equiv \sqrt{\langle x^2 \rangle_{\text{trap}}}$. This is given by $l/d_x = (l_0/d_x)(l/l_0) = (\bar{n}_0\sigma_0/\bar{n}\sigma)/(\bar{n}_0\sigma_0 d_x)$. Since the cloud size does not change, the average (density weighted) density $\bar{n}$ scales as N, and $\sigma \propto 1/U$, so the ratio scales as U/N. Hence, we have

$$\frac{l}{d_x} = \frac{N_0 U}{N U_0} \frac{1}{n_0 \sigma_0 d_x}. \tag{13}$$

For $\eta = 10$, $N/N_0 = (U/U_0)^{0.19}$. Thus, to achieve $l > d_x$ we require $(U/U_0)^{0.81} \geqslant n_0 \sigma_0 d_x$. Since l/d_x scales as $(U/U_0)^{0.81}$, the mean free path decreases almost linearly with trap depth.

Using the above results, we can write $n_0 \sigma_0 d_x \equiv U_l/U_0$, where

$$U_l = \frac{2}{\sqrt{\pi}} \frac{\lambda \eta \hbar^2 N_0}{M a_x a_y}. \tag{14}$$

Here, $\lambda = \omega_z/\omega_x = 0.035$. We use $\sigma_0 = 4\pi\hbar^2/(MU_0)$ for a Fermi gas in a 50–50 mixture, and N_0 the total atom number. For our trap conditions, we find $U_l = 12.7\,\mu\text{K}$. Hence, the evaporating atoms scatter with atoms in the trap when $U_c/U_0 \leqslant (12.7/500)^{1.23} = 0.011$. Thus, we expect that the trap can be lowered by a factor of $\simeq 100$ before the evaporation starts to become hydrodynamic.

The very good agreement between the scaling law predictions and the data for even lower trap depths suggests that the value of $\eta \simeq 10$ is nearly constant even as the evaporation becomes hydrodynamic and slows down. There is a mitigating factor which may explain this behaviour. We note from equation (9) that the evaporation rate is suppressed by a Boltzmann factor $\exp(-\eta)$. Hence, a decrease in the evaporation rate can be compensated by a small reduction in η, for example $\eta = 9.5$ increases the evaporation rate by a factor of 1.6 compared to $\eta = 10$. Thus, it is not too surprising that η can remain nearly constant until degeneracy is attained.

6. Summary

We have measured the scaling laws for the number and cloud size for forced evaporation of a unitary gas in an optical trap. By reducing the trap depth using a lowering curve which maintains a

fixed large ratio η of the trap depth to the average thermal energy, we find that atom loss is reduced and high efficiency is achieved in Fermi gases which have small inelastic losses. The value of $\eta = U/(k_B T) \simeq 10$ does not seem to depend critically on the shape of the lowering curve, but the correct unitary lowering curve permits quantum degeneracy to be achieved with high efficiency in a fraction of second. The faster timescale is important for suppressing excess atom loss and excess heating: In two-component Fermi gases near or below the Feshbach resonance, inelastic loss and heating can arise from singlet molecular relaxation [12]. Excess heating can also arise from laser intensity noise and beam pointing noise [23, 24], and from diffractive background gas collisions, especially in traps at moderate vacuum [25]–[27].

In the degenerate regime, the Fermi energy sets the energy scale, and the classical scaling law breaks down. In this regime, Pauli blocking can suppress the collision rate and the evaporation rate. However, as noted previously, the heat capacity of a degenerate Fermi gas $\rightarrow 0$ as the temperature is lowered, making the gas easier to cool [14] and obviating the effects of Pauli blocking. At low temperatures, where the unitary Fermi gas is a superfluid, the heat capacity decreases with temperature much faster than for a normal fluid, further improving the cooling rate.

Acknowledgments

References

[1] Barrett M D, Sauer J A and Chapman M S 2001 All-optical formation of an atomic Bose–Einstein condensate *Phys. Rev. Lett.* **87** 010404

[2] Granade S R, Gehm M E, O'Hara K M and Thomas J E 2002 All-optical production of a degenerate Fermi gas *Phys. Rev. Lett.* **88** 120405

[3] Thomas J E and Gehm M E 2004 Optically trapped Fermi gases *Am. Sci.* **92** 238

[4] Kramer T, Herbig J, Mark M, Weber T, Chin C, Nageral H-C and Grimm R 2004 Optimized production of a cesium Bose–Einstein condensate *Appl. Phys.* B **79** 1013

[5] Dumke R, Johanning M, Gomez E, Weinstein J D, Jones K M and Lett P D 2006 All-optical generation and photoassociative probing of sodium Bose–Einstein condensates *New J. Phys.* **8** 64

[6] Jochim S, Bartenstein M, Altmeyer A, Hendl G, Riedl S, Chin C, Denschlag J H and Grimm R 2003 Bose–Einstein condensation of molecules *Science* **302** 2101

[7] O'Hara K M, Hemmer S L, Gehm M E, Granade S R and Thomas J E 2002 Observation of a strongly interacting degenerate Fermi gas of atoms *Science* **298** 2179

[8] Bartenstein M, Altmeyer A, Riedl S, Jochim S, Chin C, Denschlag J H and Grimm R 2004 Crossover from a molecular Bose–Einstein condensate to a degenerate Fermi gas *Phys. Rev. Lett.* **92** 120401

[9] Regal C A, Greiner M and Jin D S 2004 Observation of resonance condensation of fermionic atom pairs *Phys. Rev. Lett.* **92** 040403

[10] Zwierlein M W, Stan C A, Schunck C H, Raupach S M F, Kerman A J and Ketterle W 2004 Condensation of fermionic atom pairs near a Feshbach resonance *Phys. Rev. Lett.* **92** 120403

[11] Strecker K E, Partridge G B and Hulet R G 2003 Conversion of an atomic Fermi gas to a long-lived molecular Bose gas *Phys. Rev. Lett.* **91** 080406

[12] Bourdel T, Khaykovich L, Cubizolles J, Zhang J, Chevy F, Teichmann M, Tarruell L, Kokkelmans S J J M F and Salomon C 2004 Experimental study of the BEC-BCS crossover region in lithium 6 *Phys. Rev. Lett.* **93** 050401

[13] Kinast J, Turlapov A and Thomas J E 2005 Optically-trapped Fermi gases model strong interactions in nature *Opt. Phot. News* **16** 21

[14] O'Hara K M, Gehm M E, Granade S R and Thomas J E 2001 Scaling laws for evaporative cooling in time-dependent optical traps *Phys. Rev.* A **64** 051403(R)

[15] Luiten O J, Reynolds M W and Walraven J T M 1996 Kinetic theory of the evaporative cooling of a trapped gas *Phys. Rev.* A **53** 381

[16] Ketterle W and Van Druten N J 1996 Evaporative cooling of trapped atoms *Adv. At. Mol. Opt. Phys.* **37** 181

[17] Thomas J E, Turlapov A and Kinast J 2005 Virial theorem and universality in a unitary Fermi gas *Phys. Rev. Lett.* **95** 120402

[18] O'Hara K M, Granade S R, Gehm M E, Savard T A, Bali S, Freed C and Thomas J E 1999 Ultrastable CO_2 laser trapping of lithium fermions *Phys. Rev. Lett.* **82** 4204

[19] Bartenstein M *et al* 2005 Precise determination of ^{6}Li cold collision parameters by radio-frequency spectroscopy on weakly bound molecules *Phys. Rev. Lett.* **94** 103201

[20] Windholz L, Musso M, Zerza G and Jäger H 1992 Precise Stark-effect investigations of the lithium D1 and D2 lines *Phys. Rev.* A **46** 5812

[21] Menotti C, Pedri P and Stringari S 2002 Expansion of an interacting Fermi gas *Phys. Rev. Lett.* **89** 250402

[22] O'Hara K M 2000 Optical trapping and evaporative cooling of fermionic atoms *PhD Thesis* Duke University, unpublished

[23] Savard T A, O'Hara K M and Thomas J E 1997 Laser-noise-induced heating in far-off resonance optical traps *Phys. Rev.* A **56** 1095(R)

[24] Gehm M E, O'Hara K M, Savard T A and Thomas J E 1999 Dynamics of noise-induced heating in atom traps *Phys. Rev.* A **58** 3914

[25] Bali S, O'Hara K M, Gehm M E, Granade S R and Thomas J E 1999 Quantum-diffractive background gas collisions in atom-trap heating and loss *Phys. Rev.* A **60** R29

[26] Beijerinck H C W 2000 Rigorous calculation of heating in alkali-metal traps by background gas collisions *Phys. Rev.* A **61** 033606

[27] Beijerinck H C W 2000 Heating rates in collisionally opaque alkali-metal atom traps: Role of secondary collisions *Phys. Rev.* A **62** 063614